CARBON 89 (2015) 142–147

Available at www.sciencedirect.com

ScienceDirect

journal homepage: www.elsevier.com/locate/carbon

# Carbon nanotubes as catalysts for direct carbohydrazide fuel cells

Ji Qi [a,1], Neeva Benipal [a,1], David J. Chadderdon [a], Jiajie Huo [a], Yibo Jiang [b], Yang Qiu [a], Xiaotong Han [a], Yun Hang Hu [c], Brent H. Shanks [a], Wenzhen Li [a,d,*]

[a] Department of Chemical and Biological Engineering, Biorenewables Research Laboratory, Iowa State University, Ames, IA 50011, United States

[b] Department of Civil & Environmental Engineering, Michigan Technological University, Houghton, MI 49931, United States

[c] Department of Materials Science and Engineering, Michigan Technological University, Houghton, MI 49931, United States

[d] Ames Laboratory, USDOE, Ames, IA 50011, United States

ARTICLE INFO

*Article history:*
Received 6 January 2015
Accepted 10 March 2015
Available online 16 March 2015

ABSTRACT

As an alternative to potentially carcinogenic hydrazine for fuel cell application, carbohydrazide, which contains lone electron pairs on nitrogen atoms and readily activated N–H bonds, can be catalytically oxidized over metal-free carbon catalysts due to the high equilibrium electromotive force (1.65 V) of its oxidation reaction. Carbon nanotubes are found to electrochemically catalyze the carbohydrazide oxidation reaction more efficiently than carbon black and multi-layer graphene in alkaline media. With carbon nanotubes as the anode catalyst, anode metal-catalyst-free and completely metal-catalyst-free direct carbohydrazide anion exchange membrane fuel cells are shown here to generate a peak power density of 77.5 mW $cm^{-2}$ and 26.5 mW $cm^{-2}$, respectively.



## 1. Introduction

As an abundant, stable and low-cost material, carbon is an ideal non-metal candidate for fuel cell electrocatalysts. For the realization of a low-temperature fuel cell with metal-free catalysts, active chemicals have to be adopted to overcome the overpotential barrier and thus increase the cell operating voltage. Carbohydrazide, a high energy density (4.16 kWh/L) hydrazine derivative containing readily activated N–H bonds, is a non-toxic alternative to hydrazine, and can potentially be fully oxidized to non-toxic nitrogen, water and carbon dioxide, releasing eight electrons per molecule. In acid electrolyte [1], nitrogen serves as the main product for carbohydrazide oxidation reaction (CBOR) on the platinum electrode for the reason that the stable N–N bond prevents generation of detectable toxic cyanamide and cyanate. Similarly in alkaline medium [2], the N–N bond is hard to cleave on various kinds of mono-metallic electrodes, such as Pt, Au, Ag, Fe, Co, Ni, and Cu. Moreover, the relatively high thermal-equilibrium potential (+1.65 V) of a direct carbohydrazide fuel cell at standard conditions effectively counteracts the overpotential of electrocatalytic CBOR.

In the present work, the feasibility of a novel direct carbohydrazide fuel cell powered by carbon catalysts is shown. Carbon nanotubes (CNT) outperform carbon black (CB) and multi-layer graphene (MLG) for the anodic CBOR.

* *Corresponding author at:* Department of Chemical and Biological Engineering, Biorenewables Research Laboratory, Iowa State University, Ames, IA 50011, United States.
E-mail address: wzli@iastate.edu (W. Li).

[1] Ji Qi and Neeva Benipal contributed equally to this work.

http://dx.doi.org/10.1016/j.carbon.2015.03.029
0008-6223/

An anode metal-catalyst-free direct carbohydrazide anion exchange membrane fuel cell (AEMFC) with a CNT anode catalyst and a Fe-based cathode catalyst generates a peak power density of 77.5 mW $cm^{-2}$ at 80 °C, while a completely metal-catalyst-free cell with a CNT anode catalyst and a nitrogen-doped CNT (N-CNT) cathode catalyst generates a peak power density of 26.5 mW $cm^{-2}$.

## 2. Experimental section

### 2.1. Chemicals

The short multi-walled CNT (8–15 nm outer diameter, 0.5–2 μm length), bought from Cheaptubes Inc., were grown by combustion chemical vapor deposition (CCVD) method and acid purified. They were subsequently shortened using an extrusion system.

XGnP MLG, Vulcan XC-72R CB and N-CNT were purchased from XG sciences, Inc., Fuel Cell Store and Nano Tech Labs. Inc. (NTL), respectively. Carbohydrazide (98%), polytetrafluoroethylene water solution (60%), potassium hydroxide (85%) and 1-propanol (99.5%) were obtained from Sigma–Aldrich Co. The catalyst 4020 was bought from Acta, Inc.

### 2.2. Transmission electron microscopy (TEM), Brunauer–Emmett–Teller (BET) surface area, and thermogravimetric analysis (TGA) physical characterizations

TEM images of the CNT, CB and MLG were obtained on a JEOL 2010, operated at a voltage of 200 kV. Before dropwise addition onto the copper grid support with carbon film, the samples were well-dispersed ultrasonically in methanol. BET surface area was determined by $N_2$ physisorption in a Micromeritics ASAP 2020 after a degassing process. Thermal gravimetric analysis (TGA) was performed in a Perkin Elmer STA 6000 Simultaneous Thermal Analyzer with a temperature ramp of 10 K/min and an air flow of 20 ml/min.

### 2.3. Acid purification of CNT and N-CNT and their inductively coupled plasma optical emission spectrometry (ICP-OES) characterization

The CNT and N-CNT were ultrasonicated in 3.0 M hydrochloric acid with mechanical stirring for 12 h, followed by rinsing with 6 L de-ionized water. After this process was repeated, the CNT and N-CNT were dried in a vacuum oven for 12 h. For ICP-OES analysis, the CNT and N-CNT were dissolved in aqua regia with ultra-sonication for 1 h, followed by standing overnight to promote Fe ionization. The samples were diluted to <10 ppm and then filtrated to remove carbon before Fe quantification.

### 2.4. Electrochemical characterization in three electrode half cell system and membrane electrode assembly based single cell system

The cyclic voltammetry (CV) was conducted in a traditional three-electrode, water jacket integrated glass cell (AFCELL3, Pine Instrument) with a glassy carbon working electrode (AFE3T050GC, Pine Instrument), a Hg/HgO reference electrode (MMO, CHI152, CH Instruments), and a platinum wire counter electrode (AFCTR1, Pine Instrument). 2.7 mg catalyst was dispersed in 5.4 mL 1-propanol by continuously shaking the container in an ultrasonic ice-water bath for 2 min to obtain a uniform black colored catalyst ink with a concentration of 0.5 mg $mL^{-1}$. 20 μL of the catalyst ink was added dropwise onto the surface of the glassy carbon electrode (GCE) with a glass syringe. The electrolyte was composed of 1.0 M potassium hydroxide (KOH) and 0.1 M carbohydrazide ($CH_6N_4O$). The CV tests were executed at room temperature under nitrogen protection with a scan rate of 50 mV $s^{-1}$.

The current, potential and power density raw data were collected under ambient pressure and at various temperatures on a fuel cell test stand (850e Scribner-Associates) connected with a single cell module including a self-made membrane electrode assembly (MEA), two serpentine graphite flow field plates, two glided plate-shaped current collectors and feedback temperature control loop composed of electric heating rods and thermocouple thermometer. The 5 $cm^2$ MEA was assembled by combining the anode catalyst substrate (carbon cloth), the cathode catalyst substrate integrated with membrane (A901 anion exchange membrane Tokuyama, 10 μm) and the cathode backing layer (carbon paper). The anode catalyst ink, using 1-propanol as solvent and 5% polytetrafluoroethylene (PTFE Teflon) as binder (catalyst:PTFE = 8:2 mass ratio), was ultra-sonicated in an ice-water bath for 40 min to ensure uniform dispersion even under a relatively high ink concentration of 10 mg $cm^{-3}$. The catalyst loading on the anode catalyst substrate was controlled to 10 mg $cm^{-2}$ by gradually spraying catalyst ink onto the carbon cloth. The cathode catalyst substrate was made by spraying 1 mg $cm^{-2}$ of the cathode catalyst (4020 Acta or N-CNT) onto an anion exchange membrane (A901 Tokuyama). The cathode catalyst ink was prepared similarly as the anode catalyst ink with 30 wt% of ionomer (AS4 Tokuyama) as binder and anion conductor. The default testing condition was anode fuel: 6.0 M KOH, 1.0 M carbohydrazide, 4.0 ml $min^{-1}$; cathode fuel: 200 ml $min^{-1}$ $O_2$, ambient pressure; temperature (anode fuel/cathode fuel/cell): 25/80/80 °C.

## 3. Results and discussion

The MLG have a μm-scale two-dimensional structure (diameter > 1 μm) with a flat surface (Fig. 1a), leading to a BET surface area (125 $m^2$ $g^{-1}$) lower than that of CB (254 $m^2$ $g^{-1}$) and CNT (233 $m^2$ $g^{-1}$). When MLG is fabricated into an electrode, only the surface layers are exposed to the electrolyte, leading to a remarkable amount of graphite layers buried underneath, which are inaccessible to the electrocatalytic CBOR. The CB (Vulcan XC-72R) has a much smaller diameter (Fig. 1b) than that of MLG. It can form a nm-scale rough surface when piled as catalyst layer on the electrode, enabling a higher graphite layer utilization. When the 1-D CNTs (Fig. 1c) formed random agglomeration in the catalyst layer, there is significant interspace formed between them, which provides the entire CNT-based electrode with a three-dimensional (3D) structure. Since the diameter of the CNT is only 8–15 nm, the 3D

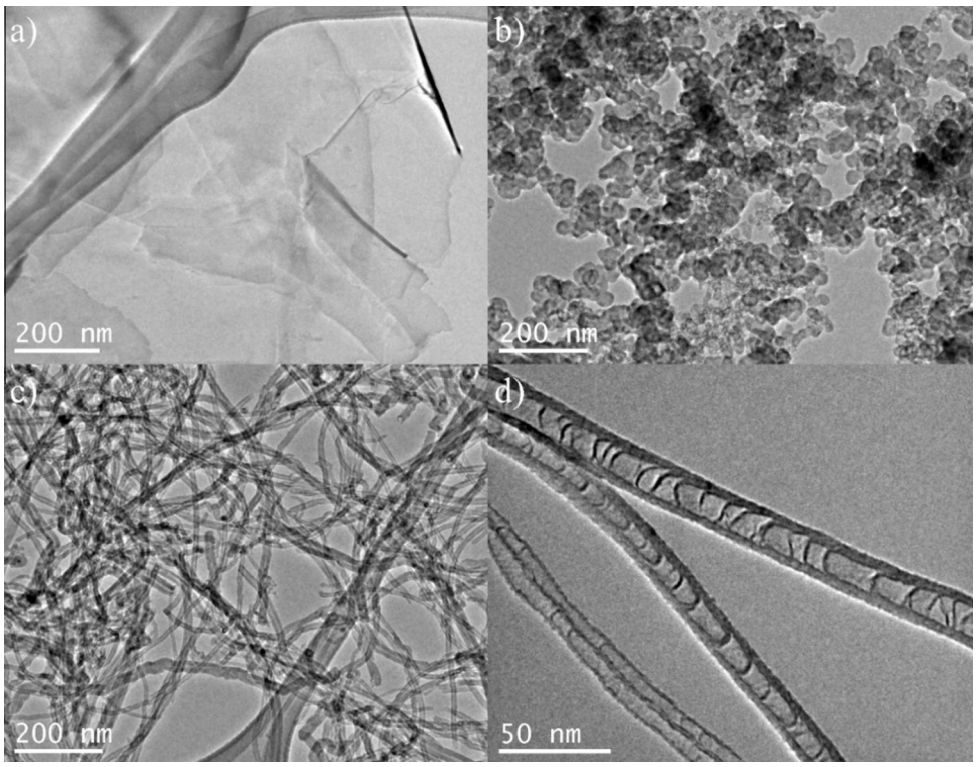


**Fig. 1 – Morphology comparison based on TEM images of (a) MLG (b) CB (Vulcan XC-72R) (c) CNT and (d) N-CNT.**

network electrode structure will ensure colossal nano-scale exposure of carbon surface to electrolyte. Despite the large BET surface area determined by gas physical adsorption, the CB has more nm-scale pores on its surface, which will likely lead to more mass transfer issues for CBOR compared with CNT. Therefore, the CNT's actual carbon surface utilization for CBOR can still be higher than that of Vulcan XC-72R. All the carbon materials are thermally stable (Table 1) in air for low-temperature anion exchange membrane fuel cell (25–90 °C).

As an azotic ligand with lone pairs of electrons with strong reducing ability [3], carbohydrazide has been proven to be electrochemically active on metal-based structures [2,4]. To evaluate the electrocatalytic activity of carbon toward carbohydrazide oxidation reaction (CBOR), cyclic voltammetry was conducted in three electrodes system with CNT, CB and MLG as catalyst on the working electrode, respectively (Fig. 2). The current density at 0.2 V for CNT (93.5 mA $cm^{-2}$) is 1.3 times that of CB (74.1 mA $cm^{-2}$), 3.8 times that of MLG (19.6 mA $cm^{-2}$) and 12.2 times that of blank glassy carbon electrode (7.1 mA $cm^{-2}$), which is attributed to the aforementioned catalyst layer structure difference of CNT (nano-scale 3D network), CB (nano-scale rough surface), MLG (micro-scale flat surface), and blank glassy carbon electrode (bulk flat surface). Due to a compromise between a small particle effect and the 3D network structure effect, the onset potential of the CBOR occurred on CB electrode (−0.440 V) is close to the counterpart for CNT (−0.420 V). With a micro-scale flat surface, the onset potential of MLG (−0.320 V) is 120 mV and 100 mV more positive than that of CB and CNT, respectively, making the dimension of catalyst a determining factor for the mass activity of carbon catalyzed CBOR in alkaline media.

Low-temperature AEMFC is adopted here as a promising platform to develop fuel cells with metal-free catalysts since reaction kinetics can be improved at both anode and cathode as a result of enhanced charge and ion transfer in high pH media. Fig. 3a–c depicts the AEMFC performance with anode metal-free carbon catalyst and cathode noble metal-free Fe-

**Table 1 – Summarization of physical characterizations for carbon materials.**

| Carbon samples | Diameter[a] (nm) | BET surface area ($m^2$ $g^{-1}$) | Thermally unstable temperature in air[b] (°C) |
|---|---|---|---|
| MLG | >1000 | 125 | 201 |
| CB | 20–50 | 254 | >400 |
| CNT | 8–15 (length: 0.5–2 μm) | 233 | 275 |
| N-CNT | 20–40 (length: ~50 μm) | 124 | >400 |

[a] Outer diameter for CNT and N-CNT; particle diameter for CB; cluster diameter for MLG.
[b] The temperature when a carbon sample loses 0.5 wt% of its original weight in TGA experiments.

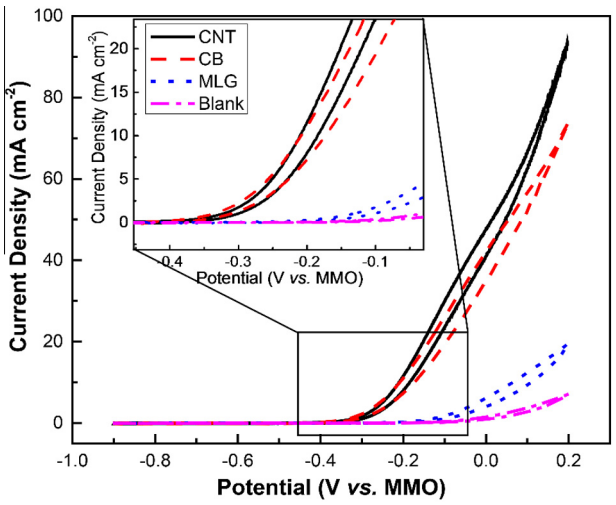


**Fig. 2 – Cyclic voltammograms of CNT, CB (Vulcan XC-72), MLG, and glassy carbon substrate for carbohydrazide oxidation in $N_2$ purged 2.0 M KOH + 1.0 M carbohydrazide at 50 mV $s^{-1}$ scan rate under room temperature. (A color version of this figure can be viewed online.)**

based (Acta 4020) catalyst, confirming the overpotential of CBOR on carbon anode catalysts is also low enough to actually generate electricity in AEMFC. As demonstrated in Fig. 3a, the open circuit voltage (OCV) of the direct carbohydrazide AEMFC with CNT as the anode catalyst is 0.630 V, which is 31 mV, 57 mV and 86 mV higher than that with CB, MLG and carbon cloth substrate, respectively. Comparable to the performance of $H_2$-AEMFC with the Ni-Cr anode catalyst and Ag cathode catalyst (50 mW $cm^{-2}$) [5], the peak power density (PPD) of the direct carbohydrazide AEMFC with CNT as the anode catalyst is 77.5 mW $cm^{-2}$, which is 11.8% higher than that with CB (69.3 mW $cm^{-2}$), 86.7% higher than that with MLG (42.2 mW $cm^{-2}$), and 5.4 times that with the blank carbon cloth substrate (12.2 mW $cm^{-2}$). Ideally, the BET surface area of carbon materials measured by gas adsorption should be proportional to the active sites exposed to electrolyte catalyzing carbohydrazide oxidation. As far as the performance of direct carbohydrazide fuel cell with CNT and MLG anode catalysts is concerned, the peak power density (77.5 mW $cm^{-2}$ and 42.2 mW $cm^{-2}$) of the AEMFCs is proportional to the BET surface area of the anode catalysts (233 $m^2$ $g^{-1}$ and 125 $m^2$ $g^{-1}$), which is not the case as for CB.

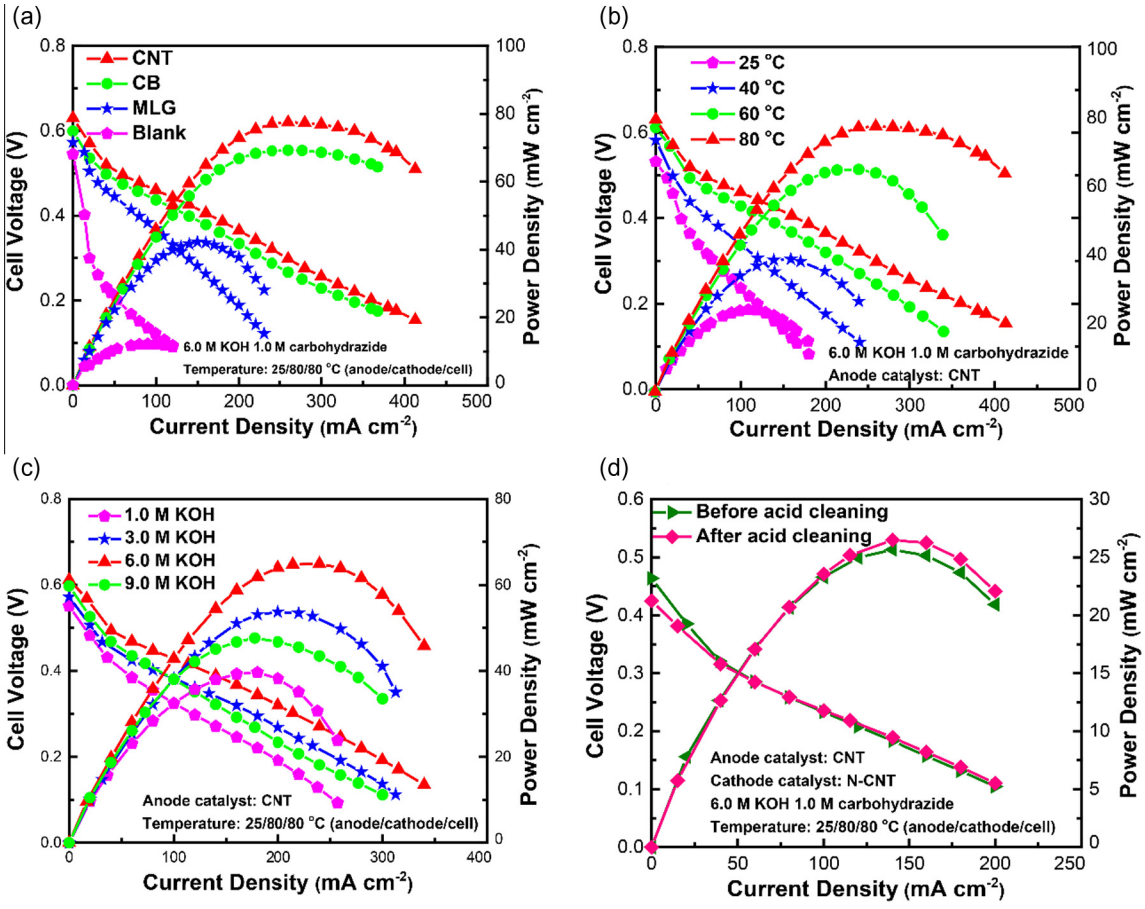


**Fig. 3 – I–V polarization and power density curves of AEMFCs with carbon anode catalyst and Fe-based Acta 4020 cathode catalyst (a–c), (a) comparison of different carbon material as anode catalyst; (b) temperature effects (c) KOH concentration effect and (d) completely metal-catalyst-free AEMFC with CNT anode and N-CNT (before or after acid cleaning) cathode catalyst. $O_2$ is fed to cathode at ambient pressure. (A color version of this figure can be viewed online.)**

The CB has more pores [6] on its surface than CNT and MLG do, so some of its active sites' effectiveness toward catalyzing carbohydrazide oxidation reaction is undermined by mass transfer issue. According to consistent results shown in both half cell and single cell tests, the mass activity sequence toward CBOR for direct carbohydrazide AEMFC application is CNT (8–15 nm) > CB (30–40 nm) > MLG (>1 μm) > bulk carbon substrate (glassy carbon or carbon cloth).

Fig. 3b shows the polarization and power density curves of direct carbohydrazide AEMFC with the CNT anode catalyst operated under different temperatures. The OCV of the anode metal-catalyst-free direct carbohydrazide AEMFC operating at 25 °C, 40 °C, 60 °C and 80 °C is 0.53 V, 0.58 V, 0.61 V and 0.63 V, while PPD is 23.9 mW $cm^{-2}$, 38.7 mW $cm^{-2}$, 64.9 mW $cm^{-2}$ and 77.5 mW $cm^{-2}$ respectively. Higher fuel cell performance can be traced back to enhanced carbohydrazide oxidation kinetics offered by elevated temperature.

As shown in Fig. 3c, the cell voltage first increases with KOH concentration up to 6.0 M and then decreases upon further concentration increases to 9.0 M. As a major factor affecting the AEMFC performance [7,8] and product distribution [9], KOH concentration has a similar parabolic relationship with single cell PPD in direct ethanol [7] and glycerol [8] AEMFC, indicating the existence of common effects. Higher KOH concentration facilitates the deprotonation of carbohydrazide and thus enhances the kinetics of carbohydrazide oxidation. Meanwhile, boosted competitive adsorption between carbohydrazide and hydroxyl ion leads to a shortage of carbohydrazide on the catalyst surface. The trade-off between enhanced kinetics and competitive adsorption has a direct association with the existence of optimized KOH concentration. Moreover, the internal resistance, which will first decrease and then increase as KOH concentration increases [8], is also responsible for the volcano type relationship between KOH concentration and single cell performance.

Fig. 3d presents the performance of total metal-catalyst-free direct carbohydrazide AEMFC, in which the cathode Fe-based Acta 4020 catalyst was replaced by N-CNT. It's reported that the residual metal on CNT has remarkable effects on biological [10] and electrochemical reactions [11]. Therefore, it is important to determine the dominant catalytic material in the current fuel cell. After purifying the anode CNT and cathode N-CNT catalyst by ultrasonication with 3.0 M hydrochloric acid (non-oxidizing acid to protect the carbon shell), the performance of the single cell before and after such process is compared, since residual Fe metal may also contribute to CBOR or ORR. By conducting hydrochloric acid treatment, the Fe amount detected by ICP-OES in anode CNT decreased from 0.019 wt% to 0.007 wt% (0.7 μg Fe $cm^{-2}$), while that in the cathode N-CNT decreases from 5.6 wt% to 0.079 wt% (7.9 μg Fe $cm^{-2}$). The one to two magnitude drop of the residual metal amount in CNT and N-CNT confirms the effectiveness of the purification process. The OCV before acid treatment is 39 mV larger than that after acid treatment while the PPD of the former MEA (26.5 mW $cm^{-2}$) is just 0.9 mW $cm^{-2}$ higher than that of the latter MEA (25.6 mW $cm^{-2}$). The metal-catalyst-free fuel cell with a MEA composed of acid purified catalysts performs similarly in electricity generation compared to one with an MEA composed of non-purified catalysts, indicating the dominant effective catalytic material is carbon rather than metal. Another reason for carbon atoms as proposed active sites is that the lone pairs of electrons make nitrogen atoms easily adsorbed. The target reaction mechanism is complete electrocatalytic oxidation of carbohydrazide with C–N bond cleavage, releasing 8 electrons per molecule:

$$CH_6N_4O + 8OH^- \rightarrow CO_2 + 7H_2O + 2N_2 + 8e^- \quad E^o = -1.25\ \text{V vs SHE} \tag{1}$$

$$2O_2 + 4H_2O + 8e^- \rightarrow 8OH^- \quad E^o = +0.40\ \text{V vs SHE} \tag{2}$$

$$CH_6N_4O + 2O_2 \rightarrow CO_2 + 3H_2O + 2N_2 \quad E^o = +1.65\ \text{V} \tag{3}$$

However, due to high activity of carbohydrazide, chemical decomposition to hydrogen is possible, which has already been reported for hydrazine [12]. Therefore, designing more active catalytic materials as well as suppressing the chemical decomposition of carbohydrazide in alkaline media can further increase the efficiency of the fuel cell.

## 4. Conclusions

In summary, we have demonstrated CNT as an active carbon-based catalyst for anode metal-catalyst-free and completely metal-catalyst-free direct carbohydrazide AEMFC. Owing to its 3D catalyst layer structure, CNT is superior to CB and MLG and toward CBOR in half cell and single cell. With CNT as anode catalyst, the PPD under optimized KOH concentration and temperature of the anode metal-catalyst-free direct carbohydrazide AEMFC with Fe-based cathode catalyst is 77.5 mW $cm^{-2}$, while the counterpart of completely metal-catalyst-free direct carbohydrazide AEMFC with N-CNT cathode catalyst is 26.5 mW $cm^{-2}$. Carbon materials with relatively smooth surface such as CNT and MLG are less affected by mass transfer issue when catalyzing CBOR. Therefore, the PPD of direct carbohydrazide fuel cell with CNT and MLG anode catalysts is proportional to the BET surface area of such carbon materials, which is the case for porous carbon such as CB. Due to the active lone pairs of electrons on nitrogen atoms of carbohydrazide molecule, carbon atoms are proposed to be active sites for CBOR, which is also evidenced by the close single cell performance before and after the acid purification of catalysts.

The preliminary confirmation of CNT powered direct carbohydrazide fuel cell provides an optional future form of fuel cells. Future work should focus on the efficiency and durability of the fuel cell from an application point of view, and on the reaction mechanism from a scientific one.

## Acknowledgements

This work is partly supported by the National Science Foundation (CBET-1159448) and Iowa State University startup fund. W. Li thanks Richard Seagrave Professorship's support, and J. Qi is grateful to the financial support from the Chinese Scholarship Council.

## REFERENCES


[1] Climent V, Rodes A, Orts JM, Feliu JM, Aldaz A. The electrochemistry of nitrogen-containing compounds at platinum single crystal electrodes – Part 3. Carbohydrazide on Pt(hkl) electrodes. J Electroanal Chem 1999;467:20–9.

[2] Asazawa K, Yamada K, Tanaka H, Taniguchi M, Oguro K. Electrochemical oxidation of hydrazine and its derivatives on the surface of metal electrodes in alkaline media. J Power Sources 2009;191:362–5.

[3] Zhang J, Zhang T, Yu K. The preparation, molecular structure, and theoretical study of carbohydrazide (CHZ). Struct Chem 2006;17:249–54.

[4] Yamazaki SI, Ioroi T, Tanimoto K, Yasuda K, Asazawa K, Yamaguchi S, et al. Electrochemical oxidation of hydrazine derivatives by carbon-supported metalloporphyrins. J Power Sources 2012;204:79–84.

[5] Lu S, Pan J, Huang A, Zhuang L, Lu J. Alkaline polymer electrolyte fuel cells completely free from noble metal catalysts. Proc Natl Acad Sci 2008;105:20611–4.

[6] Maja M, Orecchia C, Strano M, Tosco P, Vanni M. Effect of structure of the electrical performance of gas diffusion electrodes for metal air batteries. Electrochim Acta 2000;46:423–32.

[7] Li YS, Zhao TS, Liang ZX. Performance of alkaline electrolyte-membrane-based direct ethanol fuel cells. J Power Sources 2009;187:387–92.

[8] Qi J, Xin L, Zhang Z, Sun K, He H, Wang F, et al. Surface dealloyed PtCo nanoparticles supported on carbon nanotube: facile synthesis and promising application for anion exchange membrane direct crude glycerol fuel cell. Green Chem 2013;15:1133–7.

[9] Qi J, Xin L, Chadderdon DJ, Qiu Y, Jiang Y, Benipal N, et al. Electrocatalytic selective oxidation of glycerol to tartronate on Au/C anode catalysts in anion exchange membrane fuel cells with electricity cogeneration. Appl Catal B 2014;154–155:360–8.

[10] Guo L, Morris DG, Liu X, Vaslet C, Hurt RH, Kane AB. Iron bioavailability and redox activity in diverse carbon nanotube samples. Chem Mater 2007;19:3472–8.

[11] Wang L, Pumera M. Residual metallic impurities within carbon nanotubes play a dominant role in supposedly “metal-free” oxygen reduction reactions. Chem Commun 2014;50:12662–4.

[12] Sanabria-Chinchilla J, Asazawa K, Sakamoto T, Yamada K, Tanaka H, Strasser P. Noble metal-free hydrazine fuel cell catalysts: EPOC effect in competing chemical and electrochemical reaction pathways. J Am Chem Soc 2011;133:5425–31.